NANO LETTERS

2008
Vol. 8, No. 1
136−141

Controlled Fabrication and Electrical Properties of Long Quasi-One-Dimensional Superconducting Nanowire Arrays

Ke Xu and James R. Heath*

Division of Chemistry and Chemical Engineering, California Institute of Technology, MC 127-72, Pasadena, California 91125

Received September 2, 2007; Revised Manuscript Received October 30, 2007

ABSTRACT

We report a general method for reliably fabricating quasi-one-dimensional superconducting nanowire arrays, with good control over nanowire cross section and length, and with full compatibility with device processing methods. We investigate Nb nanowires with individual nanowire cross sectional areas that range from bulklike to 10 × 11 nm, and with lengths from 1 to 100 μm. Nanowire size effects are systematically studied. In particular, a comprehensive investigation of influence of nanowire length on superconductivity is reported for the first time. All results are interpreted within the context of phase-slip models.

A quasi-one-dimensional (quasi-1D) superconducting wire has a diameter less than the superconducting coherence length ξ and magnetic penetration depth λ. The Ginzburg−Landau order parameter ψ (and the density of Cooper pairs, $|\psi|^2$) becomes constant over the cross section[1,2] and is only a function of the position x along the wire. Quasi-1D superconductors provide a test-bed for investigating superconductivity in finite size. In a strictly 1D system, superconductivity is not possible.[3]

Below the superconducting transition temperature, T_c, the electrical resistance of a bulk superconductor quickly drops to zero, whereas the resistance in a quasi-1D system gradually decreases to zero. This finite resistance at $T < T_c$ is a consequence of thermally activated phase slip (TAPS) and quantum phase slip (QPS) processes.[1,4,5] For TAPS, thermodynamic fluctuations ($\sim kT$) stochastically and instantaneously depress $|\psi|$ to zero at a random point along the wire, allowing for a sudden change of 2π in the phase of ψ ("phase slip") and a finite voltage drop across the wire. The energy required to locally depress $|\psi|$ is

$$\Delta F = \frac{8\sqrt{2}}{3}\frac{H_c^{\,2}}{8\pi}A\xi \qquad (1)$$

H_c is the thermodynamic critical field and A is the cross-section area of the wire. Equation 1 represents the superconducting condensation energy within a wire segment of length $\sim\xi$ and suggests thinner wires have a smaller energy barrier for phase-slip processes and therefore a slower decrease of resistance for $T < T_c$. This can be seen from the resistance formula

$$R_{\mathrm{TAPS}} = \frac{\pi\hbar^2\Omega}{2e^2kT}\mathrm{e}^{-\Delta F/kT} \qquad (2)$$

where $\Omega = (L/\xi)(\Delta F/kT)^{1/2}(1/\tau_{\mathrm{GL}})$, L is wire length, and $\tau_{\mathrm{GL}} = \pi\hbar/8k(T_c - T)$ is the Ginzburg−Landau relaxation time. Equation 2 predicts zero resistance when T approaches zero because $kT \ll \Delta F$. Even then, however, ΔF might[5−8] be tunneled via quantum fluctuations, leading to QPS and a finite resistance when T approaches zero.

Because both $\xi(T) \approx \xi(0)(1 - T/T_c)^{-1/2}$ and $\lambda(T) \approx \lambda(0)[1 - (T/T_c)^4]^{-1/2}$ are large close to T_c, quasi-1D superconductivity was first reported in micron-size filaments within several millikelvins just below T_c.[1,2,9,10] However, for lower temperatures ξ and λ both reduce rapidly to their zero-T limits. For pure metals, $\lambda(0)$ is ~40 nm, and $\xi(0)$ varies from ~1 μm to 40 nm. Consequently, for $T < T_c$, strong quasi-1D behavior requires nanowires (NWs) with diameters substantially below 40 nm. Nontraditional fabrication methods have thus been employed, including directional deposition onto step edges,[6,8,11] sputter deposition onto suspended carbon nanotube (CNT) or DNA templates,[5,12−18] electrodeposition into porous membranes,[19−21] and etch-thinning of thick wires.[7] These experiments have together painted an incomplete picture of quasi-1D superconductors

* Corresponding author. E-mail: heath@caltech.edu.

10.1021/nl072227z CCC: $40.75
Published on Web 12/06/2007

that is consistent with the phase-slip models, but issues such as proximity effects, the lack of four-point contacts, limited materials flexibility,[22] and limited NW dimensional control are unresolved.

We report on the controlled fabrication of quasi-1D superconducting NWs. Nearly atomically straight Nb NWs with widths ranging from bulklike to 10 nm and aspect ratios approaching 10^4 are prepared. Four-point electrical measurements indicate the NWs are uniform and defect-free, and good reproducibility is found between NWs with the same *designed* cross sections. Thinner NWs exhibit a slower relative decrease of resistance below T_c, and more pronounced contributions from QPS in the low-T limit. The ability to fabricate very long (up to 100 μm) NWs with different lengths but identical cross sections has for the first time allowed for the investigation of length's sole influence on superconductivity in NWs, which are truly quasi-1D superconductors at any temperature.

Superconducting NW arrays were prepared using superlattice nanowire pattern transfer (SNAP), which translates the atomic control over the film thicknesses of a superlattice into control over the width and spacing of metal and semiconductor NWs.[23] In this method, Pt NWs are deposited by e-beam evaporation onto the raised edges of a differentially etched edge of a GaAs/$Al_xGa_{(1-x)}$As superlattice, and then transferred onto a substrate. We initially attempted to replace Pt with the superconducting materials vanadium (V) and Nb, but those NWs were not superconducting (Supporting Information). In fact, e-beam evaporated thin *films* of V and Nb were found non-superconducting, presumably due to inflated lattice parameters.[24] Thus we prepared the superconducting NW arrays in a fashion analogous to how Si NW arrays are fabricated;[25−27] i.e., SNAP is utilized to prepare a Pt NW array mask on top of a superconducting thin film, and directional dry etching is utilized to translate the Pt NW pattern into the film to produce superconducting NWs. Superconducting materials are in general not as stable as Si, so the protocol used for Si was modified accordingly. In particular, the superconducting film was protected with a thin SiO_2 layer deposited prior to the SNAP procedure. This layer also ensured the superconducting NWs were well-insulated from the Pt NW mask. The resultant on-chip NWs can be readily integrated with microcircuits on the same substrate (e.g., four-point contacts made out of either the same superconducting film or from a different material; see Supporting Information), in comparison with other methods where NWs are obtained as suspended[5,12−18] or embedded[19−21] structures, or on the very thin edges of substrates.[8,11] We chose Nb as a first demonstration, but the method should be generally applicable, including to high-T_c materials, as long as a thin film of the material is available. Representative images of the Nb NW arrays investigated in this study are presented in Figure 1.

The temperature-dependent resistance of the Nb NW arrays is presented in Figure 2. Low current levels were used to ensure an ohmic $V-I$ relationship (Supporting Information). Superconductivity is observed on all NW arrays (Figure 2A). Here we have followed the criterion for superconductivity used in previous NW studies, i.e., whether the resistance

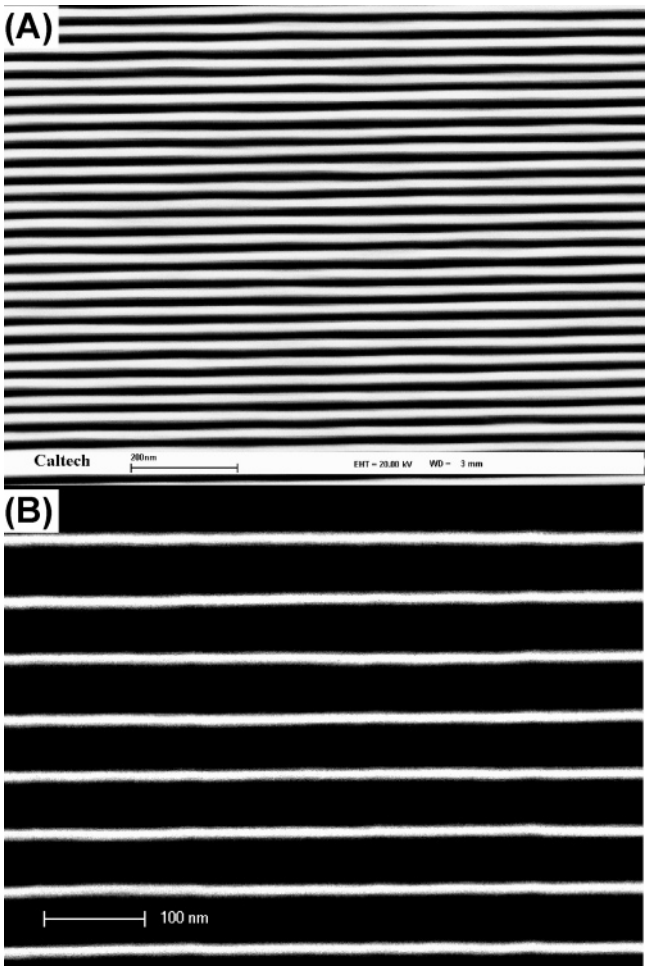

Figure 1. Scanning electron microscope (SEM) images of the NW arrays. (A) 16 nm wide NWs with 33 nm pitch (periodicity). Scale bar: 200 nm. (B) 10 nm wide NWs with 60 nm pitch. Scale bar: 100 nm. Both sets of Nb NWs are 11 nm high.

decreases significantly when the temperature is reduced below a device-dependent T_c.[5,12,13] Although not clear from Figure 2A, the thinnest NWs do show the onset of superconductivity at ~2.5 K (Supporting Information). Noticeably, superconductive behavior is observed in long (100 μm) NWs with normal-state resistance $R_N = 245$ kΩ for each individual NW. On the basis of results in short NWs, some researchers have speculated that superconductivity may not be retained in a NW if $R_N > R_q \sim 6.5$ kΩ, the quantum resistance for Cooper pairs.[12,15] This suggests that reports of observed superconductivity could be proximity-induced by superconducting contacts[28−31] and superconductivity would be difficult to retain in long (high R_N) NWs. In agreement with recent experiments,[5,8] our results indicate $R_N > R_q$ should not be the criterion for the superconductor-insulator transition in NWs.

We also examined NW arrays contacted with normal-state leads (Figure 2B). The superconductivity is partially suppressed ($T_c \sim 3.5$ K as compared with $T_c \sim 5$ K for Nb-contacted NWs of similar dimensions). The shorter NW array has a lower T_c due to higher suppression from the contacts. A residual resistance of 18 Ω is obtained for both arrays, indicative of a contact-localized superconducting-normal

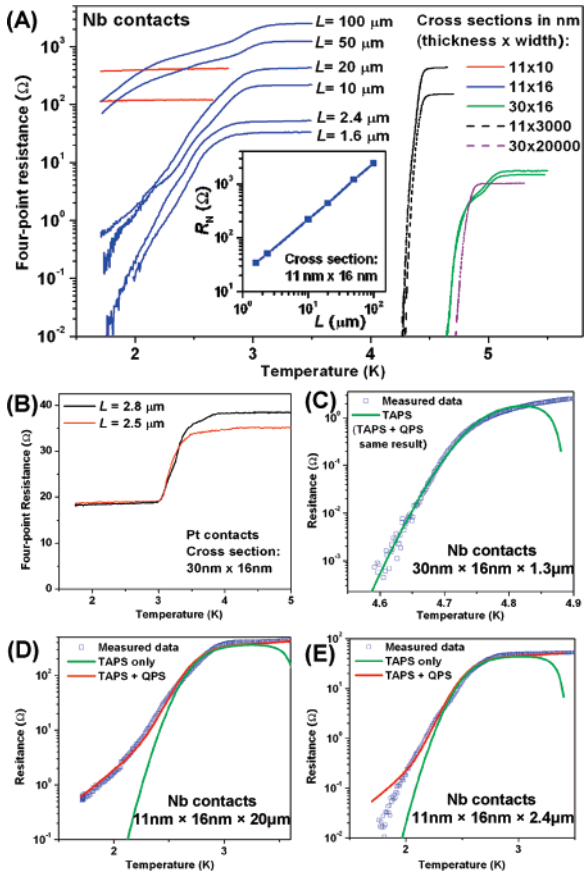

Figure 2. Temperature dependence for the four-point resistance of Nb NW arrays and films. (A) Superconducting Nb contacted NW arrays and films. Red lines: arrays of 12 NWs of cross section 11 nm × 10 nm and length L (from top to bottom) = 3 and 0.9 μm. Blue lines: arrays of 100 NWs of cross section 11 nm × 16 nm and L = 100, 50, 20, 10, 2.4, and 1.6 μm. Green lines: arrays of 250 NWs of cross section 30 nm × 16 nm and L = 1.5 and 1.3 μm. Black dashed lines: 11 nm thick films with width of 3 μm, L = 60 and 20 μm. Purple dashed line: a 30 nm thick film with width of 20 μm, L = 2.5 μm. Inset: Length dependence of the normal-state resistance for arrays of 100 NWs of cross section 11 nm × 16 nm. (B) Normal-state Pt contacted NW arrays of cross section 30 nm × 16 nm. (C) 30 nm × 16 nm × 1.3 μm data in (A) fitted to TAPS theory (TAPS + QPS gives an indistinguishable result). (D) 11 nm × 16 nm × 20 μm data fitted to the theories. (E) 11 nm × 16 nm × 2.4 μm data fitted to the theories.

mixed state.[32] To avoid contact-suppression of T_c we focused our experiments on Nb-contacted arrays.

Note from Figure 2 the consistency, for both T_c and the log(R)−T slopes, between data collected from different arrays with the same NW cross sections. The qualitatively different behavior found in the two longest arrays will be discussed later. Data from different cross section NWs are clearly different. A lower T_c is found for thinner NWs, with the cross-section dependence of T_c in general agreement with data on CNT-templated NWs.[14] According to eqs 1 and 2, the log(R)−T slope ($\sim\Delta F$) is proportional to A but independent of L. Consequently, the similar slopes in the four 11 nm × 16 nm arrays of varying lengths testify to the uniform cross section of the NWs. Moreover, the slope for these NW arrays is ~3-fold smaller than for the 30 nm × 16 nm arrays.

Three representative sets of the measured $R(T)$ data are fitted to theories. According to eq 2, $\log(R_{TAPS}) \sim -\Delta F/kT$. Because $H_c \sim (T_c - T)$ and $\xi \sim (T_c - T)^{-1/2}$, eq 1 gives $\Delta F \sim (T_c - T)^{3/2}$. This means a higher ΔF and therefore a faster drop in $\log(R_{TAPS})$ at lower T. This behavior is observed in the thicker NWs (Figure 2C), and the data fit well to TAPS theory.[5]

Thinner NW arrays deviate from TAPS fits by having resistance higher than predicted in the low-T limit (Figure 2D,E). Such behavior has been previously ascribed to QPS processes,[5−8,20] i.e., the acquisition of phase slips by tunneling through ΔF. We use the formulation adapted by Tinkham to account for QPS:[5,6]

$$R_{QPS} = B\frac{\pi\hbar^2\Omega_{QPS}}{2e^2(\hbar/\tau_{GL})}e^{-a\Delta F\tau_{GL}/\hbar} \qquad (3)$$

where $\Omega_{QPS} = (L/\xi)[\Delta F/(\hbar/\tau_{GL})]^{1/2}(1/\tau_{GL})$, and B and a are fitting parameters of order unity. Because $R_{QPS} \ll R_{TAPS}$ when T is close to T_c, the contribution from QPS is unimportant in thicker NWs (Figure 2C).

In contrast, thinner NWs have wider transitions with respect to T, and $R_{QPS} \ll R_{TAPS}$ may no longer hold at low T. Because $\Delta F \sim (T_c - T)^{3/2}$ and $\tau_{GL} \sim (T_c - T)^{-1}$, $\log(R_{QPS}) \sim -a\Delta F\tau_{GL}/\hbar \sim (T_c - T)^{1/2}$ has a weaker-than-linear dependence on T and drops more slowly at low T relative to $\log(R_{TAPS})$. Therefore, R_{QPS} is expected to dominate the total phase-slip resistance in the low-T limit. Such behavior is observed in the 11 nm × 16 nm × 20 μm sample (Figure 2D). For similar but shorter NWs, an improved fit is obtained by taking into account both TAPS and QPS. However, a nearly constant log(R)−T slope is observed in the low-T limit (Figure 2E), deviating from QPS prediction. Such behavior has been reported in short NWs,[5,7,12−14] whereas long NWs typically show the expected QPS behavior,[6,8,20] in agreement with our results. Because precise control of length and cross section has been difficult in previous studies, these observations have been inconclusive. We believe our data indicate that QPS can be partially suppressed in short NWs in the low-T limit due to contact effects, e.g., a local enhancement of ψ, as will be discussed further later.

The two longest NW arrays show a wide shoulder feature around 2.5 K that cannot be explained with TAPS and QPS theories. A similar feature was recently reported in an Al NW 100 μm in length and was accounted for by assuming the NW to be composed of segments of two different cross section areas with different T_c.[8] This argument, however, cannot explain why the shoulder is not observed in an Al NW 10 μm in length[11] or in any of the $L \leq 20$ μm NW arrays with the *same* cross section in our experiment. Also, it is hard to imagine why our 50 and 100 μm long arrays of 100 Nb NWs would both contain segments of exactly *two* different cross sections such as was proposed for the single Al NW. This "abnormal" behavior of long NW arrays in comparison with the consistent results found on the other four shorter arrays implies the shoulder feature should have a sole mechanism that depends only upon the length of the NWs. This mechanism will be discussed in detail later.

Whereas low-current limit measurements reflect the equilibrium properties of the NWs, the high-current limit represents different physics, because the current itself causes the breakdown of superconductivity and so can address how large a supercurrent can be sustained in a NW (array). In addition, true quasi-1D superconductors provide for an ideal system to study the current-induced nonequilibrium phenomena.[2] However, a systematic study on this topic with varied dimensions of NWs has been lacking. In this regime, we observe three qualitatively different behaviors when the dimensions of the NWs are varied by design (Figure 3).

Strong hysteresis is found in the $V-I$ responses of thicker NWs at base temperature (Figure 3A): the transition between the superconducting and normal states happens at different current levels for decreasing and increasing current. Such hysteresis is characteristic of single NWs[8,14,17,33] but has not been observed in NW arrays before,[19−21] presumably due to the large [∼10 nm (ref 20)] NW-to-NW diameter variation. The observed clear hysteresis, as well as the fact that the I_c per NW (2.1 mA/250 = 8.4 μA) is comparable to a CNT-templated short Nb NW of similar width[14] suggests the uniformity and high quality of our NWs, so the collective behavior of the array retains the traits of individual NWs. Because we have more than 100 NWs per array, the resultant total I_c = 2.1 mA is more than 10^2 higher than those previously reported in individual NWs or small NW arrays. This large I_c in our on-chip arrays could find applications in carrying high levels of low-dissipation current, and the strong hysteresis effect could be potentially tailored into an information storage or switching mechanism with a high on−off ratio and low power dissipation. Both I_c and I_r drop when T is raised, but I_r drops slower so the hysteresis weakens and eventually disappears at high temperature (Figure 3A inset), in agreement with results on individual NWs.[17] The hysteresis is not found in the thinner NWs at low T (Figure 3B,C) due to the larger residual resistance, again agreeing with results on single NWs.[33] I_c is significantly reduced compared to the thicker NWs, consistent with previous experiments.[18]

Qualitatively different behaviors are also found for NWs with the same cross section but different lengths. In comparison with a single jump between the superconducting and normal states at I_c for shorter NWs (Figure 3B), longer NWs first enter an intermediate state at I_c, and jump to the normal state at a higher current level, $I_N \sim 2I_c$ (Figure 3C). This intermediate region exhibits multiple voltage jumps (Figure 3C inset). Such behavior is characteristic of long quasi-1D superconductors, and each voltage jump is associated with the emergence of a localized resistive "phase-slip center" (PSC) along the wire.[1,2,10] In contrast to the stochastic TAPS and QPS events, PSCs are stable and have fixed locations for a constant driving current. Each PSC occupies a characteristic length of $\sim 2\Lambda_{Q^*}$, where $\Lambda_{Q^*} \sim 10$ μm is the quasiparticle diffusion length. The number of PSCs a wire can accommodate should be $\sim L/2\Lambda_{Q^*}$. The evolution of PSCs have been extensively studied in microbridges and submicron "whiskers"[2] very close to T_c and mesoscopic (∼100 nm) nanoribbons,[34] but results on NWs, which are truly quasi-1D superconductors at any temperature, have been limited. For example, in electrodeposited Sn NW arrays, PSCs are pinned down at local defects, and the number of PSCs observed is independent of the length of the arrays.[20]

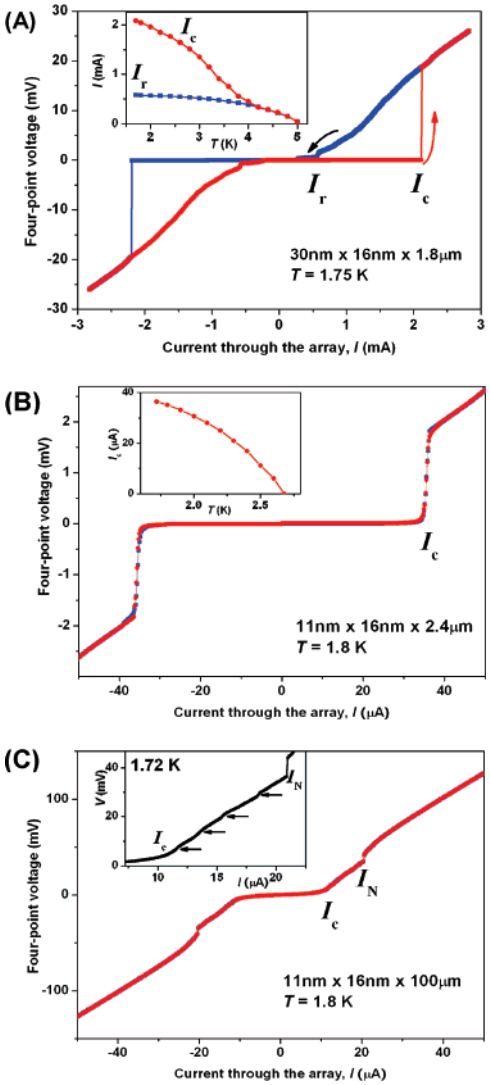

Figure 3. Four-point $V-I$ curves for three representative arrays of NWs, measured with increasing (red) and decreasing (blue) current bias at the base temperature. (A) An array of 250 NWs of cross section 30 nm × 16 nm and L = 1.8 μm. I_c denotes the critical current, i.e., the highest supercurrent that can be sustained when the applied current is swept up from zero, and I_r denotes the retrapping current, i.e., the current level at which the array returns to the superconducting state when the current is swept back down. Inset: temperature dependence of I_c and I_r. (B) An array of 100 NWs of cross section 11 nm × 16 nm and L = 2.4 μm. Inset: temperature dependence of I_c. (C) An array of 100 NWs of cross section 11 nm × 16 nm and L = 100 μm. Inset: Expanded plot of the intermediate-state region ($I_c < I < I_N$); arrows point to voltage jumps.

We have charted the evolution of PSCs in our (11 nm × 16 nm) NW arrays with L = 2−100 μm, by plotting dV/dI, so that each PSC-related voltage jump in the $V-I$ curve appears as a peak.[34] These features evolve reproducibly as a function of T and applied magnetic field (Figure 4). In the low-T limit, four and two peaks are found for L = 100 μm and L = 50 μm NWs, respectively, between I_c (∼12 μA) and I_N (∼24 μA). NWs with $L \leq 20$ μm exhibit no peak

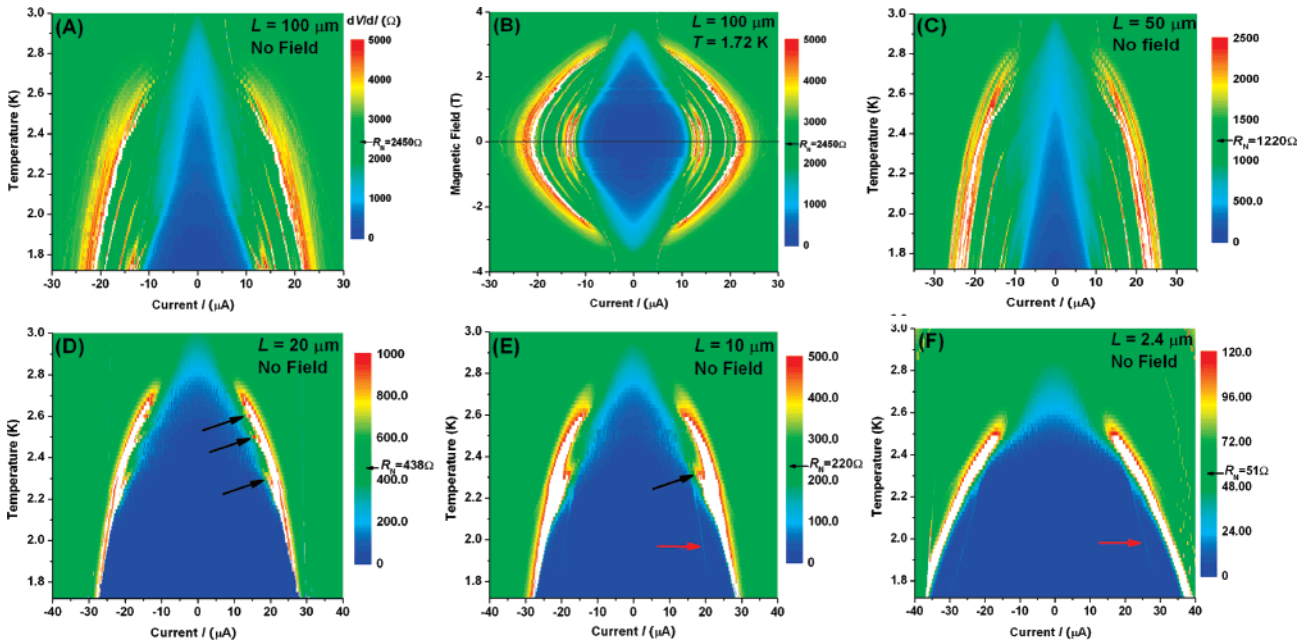

Figure 4. Differential resistance dV/dI of arrays of 100 NWs of cross section 11 nm × 16 nm, as a function of current, temperature and applied magnetic field. (A) and (C)−(F) temperature is varied at zero field. (B) Applied magnetic field is varied at constant temperature $T = 1.72$ K. The lengths of the arrays are labeled on each plot. Black arrows point to the small branching features observed close to I_c at higher temperatures for arrays of intermediate lengths, and red arrows point to the very faint (light blue) peak lines found only on the two shortest arrays.

lines. The faint features found on the two shortest arrays are attributed to contact-induced PSCs.[35] Theory predicts[1,36] that for an *absolutely uniform* filament of length L, approximately $L/2\Lambda_{Q^*}$ steps should occur between I_c and $2I_c$. The length of each PSC in our NWs can thus be estimated to be $2\Lambda_{Q^*} \sim 25\ \mu$m, comparable to the 10−50 μm values found in various materials.[10,19,37] Three small branching features are observed close to I_c for the 20 μm NWs (Figure 4D), whereas the 10 μm NWs have one such feature (Figure 4E), suggesting PSCs can still appear in NWs slightly shorter than $2\Lambda_{Q^*}$ when the energy provided by T and current is sufficiently high. Such branching is not seen in the 2.4 μm (Figure 4F) and 1.6 μm (not shown) arrays where $L \ll 2\Lambda_{Q^*}$. The clear and consistent length dependence of PSCs' behavior revealed in the above discussions supports our conclusions that the NWs are uniform and effectively defect-free (defects would act as pinning centers for PSCs). The collective behavior of 100 NWs agrees with that expected for a single homogeneous quasi-1D superconductor.[36]

The characteristic lengths revealed above should also be relevant to the equilibrium properties of the NWs. In particular, consider the shoulder feature observed at ∼2.5 K in the low-current $R-T$ curves of the 50 and 100 μm arrays. This feature deviates from TAPS and QPS models but coincides with the onset of stable PSC peak lines (Figure 4A,C). Such features are not observed in shorter NWs that exhibit no PSC peak lines in the high-current limit. NWs longer than $\sim 2\Lambda_{Q^*}$ could allow for multiple phase-slip events in each NW at the same instant. This is not considered in the TAPS and QPS models.[5,7,38] A resistance higher than predicted (i.e., the shoulder feature) would thus be observed. Shoulder features were observed in early experiments on long tin whiskers[1,9] near T_c but were attributed to contact effects,[1] which is clearly not the case for our results. As discussed earlier, the faint features found on the *shortest* arrays (Figure 4E,F) may arise from contact effects, but the corresponding local enhancement of ψ is found to suppress QPS and result in *smaller* residual resistances in comparison with theory (cf. Figure 2E and related discussions).

We have reported on the fabrication and properties of superconducting NW arrays with good control over both cross section and length. The NWs are compatible with device processing, allowing for the establishment of four-point electrical contacts. Electrical measurements in the low-current and high-current limits indicate the NWs obtained are uniform and effectively defect-free. Size effects on superconductivity are systematically studied; in particular, the ability to fabricate very long NWs with identical cross sections allows for the first systematic investigation of length's sole influence on superconductivity in NWs. The fabrication method demonstrated with Nb NWs should be broadly applicable to various thin film superconductors.

Acknowledgment. We thank Yue Zou and Wan Li (Cornell) for helpful discussions, and Kevin Kan and Hoc Ngo (UCLA Nanolab) for their assistance in device fabrication. This work was supported primarily by the Department of Energy (DE-FG02-04ER46175). Infrastructure supporting this project was supported by DARPA and by the National Science Foundation (NSF-CCF-05204490).

Supporting Information Available: Description of the fabrication processes. Supplementary Figures S1−S4 showing the process flow, SEM images, resistance measurements, $V-I$ curves, and resistance−temperature curves. This material is available free of charge via the Internet at http://pubs.acs.org.

References

(1) Tinkham, M. *Introduction to Superconductivity*, 2nd ed.; McGraw-Hill: New York, 1996.
(2) Tidecks, R. *Current-Induced Nonequilibrium Phenomena in Quasi-One-Dimensional Superconductors*; Springer-Verlag: Berlin, 1990.
(3) Mermin, N. D.; Wagner, H. *Phys. Rev. Lett.* **1966**, *17*, 1133.
(4) Little, W. A. *Phys. Rev.* **1967**, *156*, 396.
(5) Lau, C. N.; Markovic, N.; Bockrath, M.; Bezryadin, A.; Tinkham, M. *Phys. Rev. Lett.* **2001**, *87*, 217003.
(6) Giordano, N. *Phys. Rev. Lett.* **1988**, *61*, 2137.
(7) Zgirski, M.; Riikonen, K. P.; Touboltsev, V.; Arutyunov, K. *Nano Lett.* **2005**, *5*, 1029.
(8) Altomare, F.; Chang, A. M.; Melloch, M. R.; Hong, Y. G.; Tu, C. W. *Phys. Rev. Lett.* **2006**, *97*, 017001.
(9) Newbower, R. S.; Tinkham, M.; Beasley, M. R. *Phys. Rev. B* **1972**, *5*, 864.
(10) Skocpol, W. J.; Beasley, M. R.; Tinkham, M. *J. Low Temp. Phys.* **1974**, *16*, 145.
(11) Altomare, F.; Chang, A. M.; Melloch, M. R.; Hong, Y.; Tu, C. W. *Appl. Phys. Lett.* **2005**, *86*, 172501.
(12) Bezryadin, A.; Lau, C. N.; Tinkham, M. *Nature* **2000**, *404*, 971.
(13) Tinkham, M.; Lau, C. N.; Markovic, N. *Physica E* **2003**, *18*, 308.
(14) Rogachev, A.; Bezryadin, A. *Appl. Phys. Lett.* **2003**, *83*, 512.
(15) Bollinger, A. T.; Rogachev, A.; Remeika, M.; Bezryadin, A. *Phys. Rev. B* **2004**, *69*, 180503.
(16) Hopkins, D. S.; Pekker, D.; Goldbart, P. M.; Bezryadin, A. *Science* **2005**, *308*, 1762.
(17) Rogachev, A.; Bollinger, A. T.; Bezryadin, A. *Phys. Rev. Lett.* **2005**, *94*, 017004.
(18) Rogachev, A.; Wei, T. C.; Pekker, D.; Bollinger, A. T.; Goldbart, P. M.; Bezryadin, A. *Phys. Rev. Lett.* **2006**, *97*, 137001.
(19) Vodolazov, D. Y.; Peeters, F. M.; Piraux, L.; Matefi-Tempfli, S.; Michotte, S. *Phys. Rev. Lett.* **2003**, *91*, 157001.
(20) Tian, M. L.; Wang, J. G.; Kurtz, J. S.; Liu, Y.; Chan, M. H. W.; Mayer, T. S.; Mallouk, T. E. *Phys. Rev. B* **2005**, *71*, 104521.
(21) Tian, M. L.; Wang, J. G.; Kumar, N.; Han, T. H.; Kobayashi, Y.; Liu, Y.; Mallouk, T. E.; Chan, M. H. W. *Nano Lett.* **2006**, *6*, 2773.
(22) Zhang, Y.; Dai, H. J. *Appl. Phys. Lett.* **2000**, *77*, 3015.
(23) Melosh, N. A.; Boukai, A.; Diana, F.; Gerardot, B.; Badolato, A.; Petroff, P. M.; Heath, J. R. *Science* **2003**, *300*, 112.
(24) Neugebauer, C. A.; Ekvall, R. A. *J. Appl. Phys.* **1964**, *35*, 547.
(25) Wang, D. W.; Sheriff, B. A.; Heath, J. R. *Nano Lett.* **2006**, *6*, 1096.
(26) McAlpine, M. C.; Ahmad, H.; Wang, D.; Heath, J. R. *Nature Mater.* **2007**, *6*, 379.
(27) Green, J. E.; Choi, J. W.; Boukai, A.; Bunimovich, Y.; Johnston-Halperin, E.; Delonno, E.; Luo, Y.; Sheriff, B. A.; Xu, K.; Shin, Y. S.; Tseng, H. R.; Stoddart, J. F.; Heath, J. R. *Nature* **2007**, *445*, 414.
(28) Kasumov, A. Y.; Deblock, R.; Kociak, M.; Reulet, B.; Bouchiat, H.; Khodos, I. I.; Gorbatov, Y. B.; Volkov, V. T.; Journet, C.; Burghard, M. *Science* **1999**, *284*, 1508.
(29) Morpurgo, A. F.; Kong, J.; Marcus, C. M.; Dai, H. *Science* **1999**, *286*, 263.
(30) Doh, Y. J.; van Dam, J. A.; Roest, A. L.; Bakkers, E.; Kouwenhoven, L. P.; De Franceschi, S. *Science* **2005**, *309*, 272.
(31) Xiang, J.; Vidan, A.; Tinkham, M.; Westervelt, R. M.; Lieber, C. M. *Nature Nanotechnol.* **2006**, *1*, 208.
(32) Boogaard, G. R.; Verbruggen, A. H.; Belzig, W.; Klapwijk, T. M. *Phys. Rev. B* **2004**, *69*, 220503.
(33) Tinkham, M.; Free, J. U.; Lau, C. N.; Markovic, N. *Phys. Rev. B* **2003**, *68*, 134515.
(34) Falk, A.; Deshmukh, M. M.; Prieto, A. L.; Urban, J. J.; Jonas, A.; Park, H. *Phys. Rev. B* **2007**, *75*, 020501.
(35) Yeh, W. J.; Dai, Y. D.; Kao, Y. H. *J. Low Temp. Phys.* **1983**, *52*, 249.
(36) Tinkham, M. *J. Low Temp. Phys.* **1979**, *35*, 147.
(37) Liengme, O.; Baratoff, A.; Martinoli, P. *J. Low Temp. Phys.* **1986**, *65*, 113.
(38) Golubev, D. S.; Zaikin, A. D. *Phys. Rev. B* **2001**, *64*, 014504.

NL072227Z